ORGANOMETALLICS

Article

pubs.acs.org/Organometallics

Ultrarigid Indenyl-based Hafnocene Complexes for the Highly Isoselective Polymerization of Propene: Tunable Polymerization Performance Adopting Various Sterically Demanding 4-Aryl Substituents

Martin R. Machat,[†] Dominik Lanzinger,[‡] Alexander Pöthig,[§] and Bernhard Rieger*[,†]

[†]Wacker-Lehrstuhl für Makromolekulare Chemie, Technische Universität München, Lichtenbergstraße 4, 85748 Garching bei München, Germany

[‡]Advanced Materials & Systems Research, BASF SE, GCP/PM-B001, 67056 Ludwigshafen am Rhein, Germany

[§]Catalysis Research Center, Technische Universität München, Ernst-Otto-Fischer Straße 1, 85748 Garching bei München, Germany

Supporting Information

ABSTRACT: Two novel silyl-bridged C_2-symmetric (2-methyl-4-aryl-7-methoxy) substituted bisindenyl based *ansa*-hafnocene complexes of varied steric demand (**I**, 4-phenyl; **II**, 4-[(3′,5′-methyl)-phenyl]) were synthesized and examined in the coordinative polymerization of propene. Both complexes enable a comparative study with the state of the art homogeneous metallocene catalyst (**III**, 4-[(3′,5′-*tert*-butyl)-phenyl]) for high melting ultrahigh molecular weight isotactic polypropylene. All three activated complexes exhibit extremely concise stereoregularity along with high molecular weights and high melting transitions at low to moderate polymerization temperatures. Increased sterical encumbrance of the 4-aryl substituent prevents the process of chain release reactions more effectively, especially due to enhanced reduction of β-methyl elimination. Accordingly, end group analysis disclosed the highest selectivity toward allylic chain ends as a result of β-methyl elimination with the less sterically encumbered complex **I**. Examination of the catalytic activity of **I**−**III** disclosed considerable impact of the varied 4-aryl substituents on the maximum productivity with respect to the applied polymerization conditions considering the combined influence of activation, monomer diffusion rate, catalyst deactivation, and rate of chain growth.

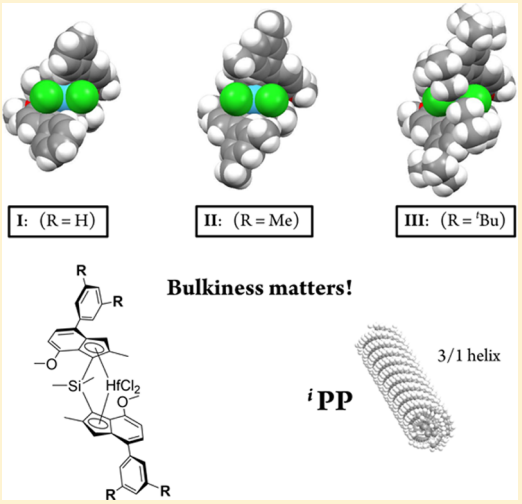

INTRODUCTION

In 1985 the first indenyl based *ansa*-zirconocene-methylaluminoxane (MAO) catalytic system for the narrow molecular weight distributed isospecific polymerization of propene was discovered by the combined work of Kaminsky and Brintzinger.[1−3] Since then vast interest aroused to optimize the polymerization performance of metallocene complexes in the single-site catalysis to polypropylene (PP).[4] Ewen's symmetry rules describing the relationship between complex symmetry and polymer microstructure were crucial for further development of complex design with respect to the desired PP properties.[5] The synthesis of polypropylenes with variable microstructures, which were not accessible using heterogenic Ziegler−Natta systems,[6,7] evoked huge scientific effort concerning polypropylene with tailored tacticities particularly comprising elastic behavior.[8−11] In 1994 Spaleck and co-workers reported the catalysis to highly isotactic polypropylene using − $SiMe_2$− bridged (2-methyl-4-phenyl) substituted *rac*-bisindenyl zirconocene complexes (SBI type) which revealed exceptional potential in the precise single-site catalysis of high molecular weight ^{i}PP.[12−16] The remarkable high molecular weights obtained with these systems activated with MAO are attributed to the effective shielding of the ligand preventing exchange reactions with $AlMe_3$ setting free the polymer chain.[17] Further strategies toward highly isoselective PP catalysis were developed using C_1-symmetric *ansa*-cyclopentadienyl(cp)-fluorenyl coordinated zirconocene complexes, titanium salen complexes and bis(phenolate) ether complexes (Zr, Hf) respectively.[18−23] While initially low activities were observed applying hafnocene complexes for the polymerization of olefins alternative activation reagents to MAO enabled the utilization of hafnocene complexes as highly productive metallocene catalysts.[24−27] In 2012 further adjustment of the primary Spaleck-type ligand structure by Schöbel et al. lead to ultrarigid metallocene complexes producing polypropylenes with ex-

Received: October 26, 2016

DOI: 10.1021/acs.organomet.6b00814
Organometallics XXXX, XXX, XXX−XXX

tremely high molecular weights and extraordinary precision with respect to the stereo- and regioselective polymerization behavior.[28] To date the resulting polymer exhibits the highest melting transition for untreated ^{i}PP (*ex reactor*) and was further investigated regarding the exceptional thermal characteristics of the almost perfect ^{i}PP polymer.[29] Just recently, the high potential in terms of catalytic activity of SBI-type metallocene complexes was reported as a result of weak electrophilic attraction of the metal center toward the respective counterion.[30,31] Calculations on related zirconocene complexes supported the additional effect of 3′,5′-substitution on the 4-phenyl substituent with respect to the stereo- and regioselectivity.[16,32] In order to gain deeper insight into the outstanding catalyst performance of these ultrarigid 2,4,7-substituted bisindenyl hafnocene complexes the focus is drawn to different 4-aryl substituents possessing a varied 3′5′-substitution pattern of decreased steric encumbrance.

RESULTS AND DISCUSSION

Syntheses. Varied ligand structures with different 4-aryl substituents were obtained starting with the literature known indene derivative **1** followed by a Suzuki cross-coupling reaction in order to implement different aryl groups in position 4 of the indenyl fragment.[28,33] Whereas **3a** and **b** react with $SiMe_2Cl_2$ in a regioselective manner after the deprotonation with ^{n}BuLi, a mixture of regioisomers regarding position 1 and 3 of the indenyl fragment was obtained with the phenyl substituted fragment. Therefore, the alternative reaction pathway **B** (Scheme 1) for the synthesis of ligand **4** was

Scheme 1. Synthesis Route to 2,4,7-Substituted Hafnocene Complexes with Varied 4-Aryl Substituents

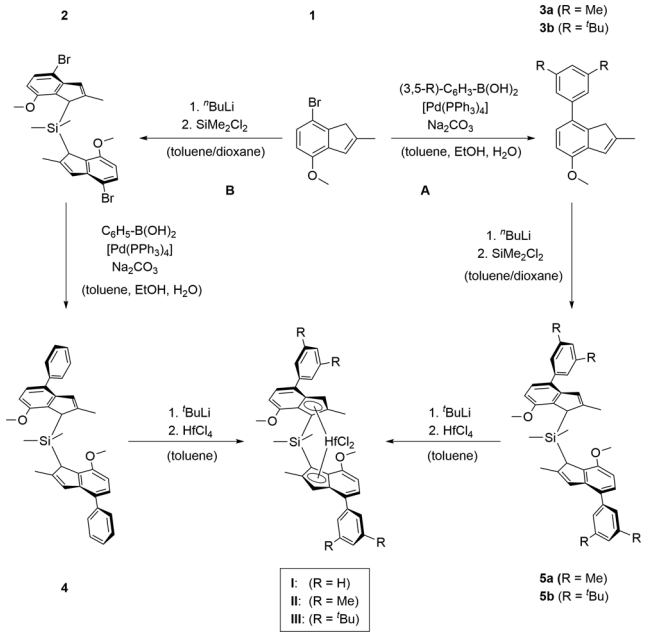

developed. The lithiated substrate **1** turned out to react with $SiMe_2Cl_2$ regioselective at position 1 of the indenyl fragment followed by a subsequent introduction of the phenyl groups. Deprotonation of ligands **4**, **5a-b** with ^{t}BuLi in toluene and the successive addition of $HfCl_4$ led to a mixture of the corresponding *racemic* and *meso* complex. Separation was conducted with different pentane/toluene mixtures at adjusted temperatures isolating the desired *rac*-hafnocene complexes **I**–**III**.

Single crystals suitable for X-ray diffraction analysis were obtained of **I** and **II** by diffusion of pentane into a saturated complex solution in toluene or benzene. Crystals of complex **I** possess an additional incorporation of 1.0 eq. of benzene. The crystal structure of complex **III** is already literature known (CCDC: 841806).[28] ORTEP style representations of **I** and **II** are given in Figure 1, important bond lengths and angles of all three complexes are depicted in Table 1.

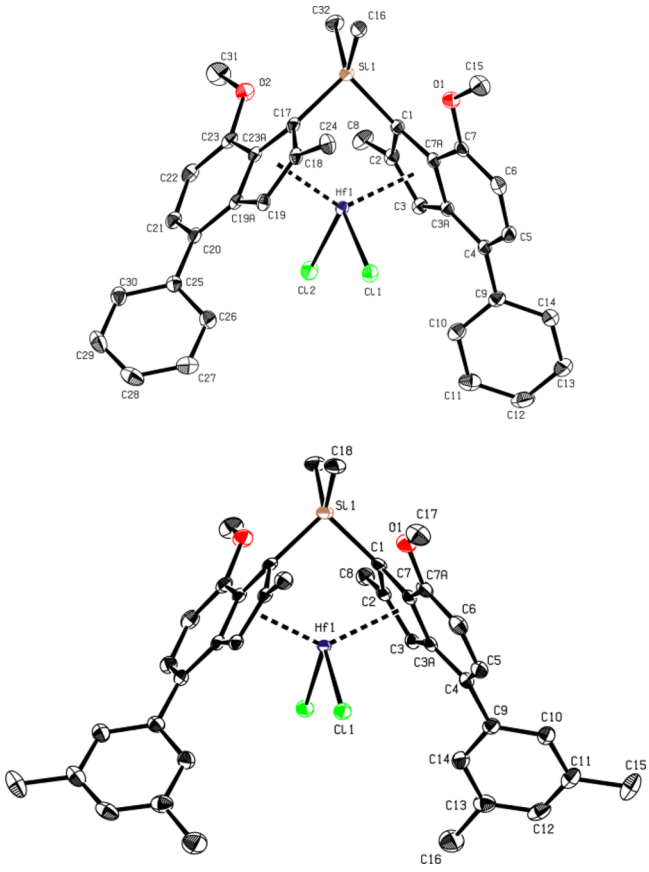

Figure 1. ORTEP style representation of **I** (top) and **II** (bottom) with ellipsoids drawn at 50% probability level. Hydrogen atoms are omitted for clarity.

In the solid state, the largest dihedral angle is observed for complex **II** possessing the largest bite angle. The shortest bond length between the central metal and the cp-center as well as the lowest D-value indicating that the metal center is less exposed to the surrounded environment, were measured in the solid state of complex **III**. Unfortunately, a consistent trend of

Table 1. Characteristic Angles and Distances of the Solid State Structures (I–III)

	bite angle[a] (deg)	dihedral angle[a] (deg)	Hf–$Cp_{centroid}$ (Å)	D^{a} (Å)
I	58.9	41.1/45.2	2.224 ± 2	0.949 ± 4
II	59.6	48.6	2.231	0.949
III[28]	57.8	42.6	2.218	0.926

[a]According to refs 34 and 35. Complex **I** differs from accurate C_2 symmetry.

DOI: 10.1021/acs.organomet.6b00814
Organometallics XXXX, XXX, XXX–XXX

bond lengths and angles with respect to an increased steric demand of the 4-aryl substituents is not observed in the solid state. The incorporation of solvent molecules in the case of **I** as well as lattice effects leading to enhanced compression especially for the ^{t}Bu-substituted complex during crystal packaging disables the opportunity to draw further conclusion regarding the chemical behavior in solution. Nevertheless, the impact of increased sterically encumbered 4-aryl substituents on the coordination gap aperture[36] is conveniently illustrated by the solid state structures (Figure 2).

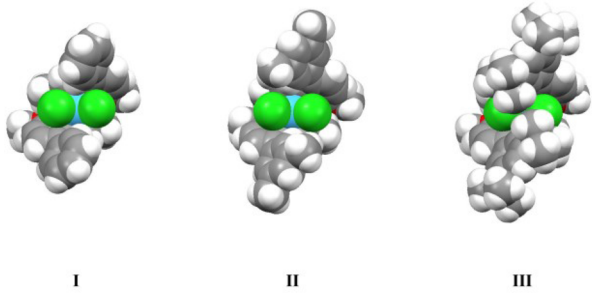

Figure 2. Space filling representation of **I**–**III** illustrating the effect of different 4-aryl substituents on the coordination gap aperture (cga).

Evaluation of geometric characteristics of the complex structures is presented based on the graphic illustration of Figure 3. All three complexes carry a methoxy substituent in

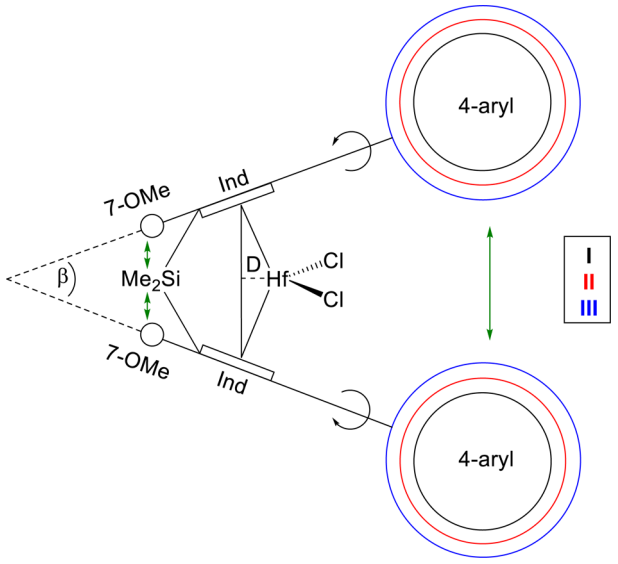

Figure 3. Graphic illustration of **I**–**III** pointing out the steric interactions leading to the rigid complex framework.

position 7 of the indenyl fragment, which is known to cause stereorigidity in the complex structure by repulsive interaction with the $-SiMe_2-$ bridge. As a consequence the bite angle is lowered.[28,37] In addition, two opposing interactions determining the conformation of the 4-aryl substituents related to the indenyl fragment are essential for the structure of these complexes. This phenomena, being partially described by the dihedral angle, is a result of reaching the energetic minimum in a coplanar structure by maximized delocalization, interfering with the reduction of steric interactions by rotation of the 4-aryl substituent. On a molecular level including rotational, vibrational and motional processes the steric interaction of the 3′,5′-substituents of both indenyl fragments tends to widen the bite angle in connection with increased steric encumbrance. This suggestion is supported by the space filling representations of Figure 2 and the schematic representation of Figure 3. The result of combined compressing and widening forces (green arrows, Figure 3) is expected to preserve the rigid complex framework in a broad temperature range.

Productivity. All three complexes were tested regarding their catalytic behavior in the polymerization of propene under identical conditions (Table 2). The activated complexes **I**-**III** are capable of producing high molecular weight and highly isotactic polypropylenes possessing high productivities. To gain detailed information on the particular catalytic activities Figure 4 visualizes essential factors determining the overall productivity.

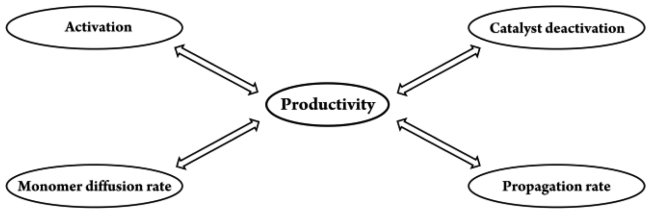

Figure 4. Main influencing factors affecting the productivity in the coordinative polymerization of olefins.

Activation of all three complexes proceeds in two steps starting with an alkylation of the bishalogenated complex using 200 eq. of triisobutylaluminum (TIBA) at 60 °C for 1 h. The cationic, catalytically active species is generated *in situ* by the addition of 5 eq. of $[Ph_3C][B(C_6F_5)_4]$. Monitoring the reaction of **I**–**III** with 200 eq. of TIBA at 60 °C via UV VIS spectroscopy indicates a fast substitution reaction due to a shift of the absorbance maxima to lower wavelength (see Supporting Information). Although the substitution reaction is much slower for complex **III** compared to **I** and **II** a distinct shift of the absorbance maxima is observed after 1 h. The reaction of $[Ph_3C][B(C_6F_5)_4]$ with alkylated metallocenes is stated to proceed quite rapid leading to the assumption that the overall activation process should be comparable for all three complexes.[24,25,38,39]

The polymers from complexes **I**–**III** produced at temperatures up to 30–50 °C almost exclusively precipitate during the polymerization therefore limiting the productivity since accessibility of further monomer units to the catalytically activated complexes is significantly reduced. In addition, during precipitation of the polymer also active catalyst may be removed from the solution. At higher polymerization temperatures the polymer remains in solution enabling higher yields in the batch process as the produced polymer is acting as additional viscous solvent during the polymerization reaction. Hence, the averaged chain length as well as the stereo- and regioregularity of the polymer are crucial for the viscosity of the reaction mixture in addition to the total amount of produced polymer. In general, enhanced viscosity reduces the productivity since diffusion of monomer to the metal center is rather limited. Due to the direct relation of viscosity and polymer formation the diffusion rate is particularly lowered at longer reaction times. Thus, the amount of catalyst is adjusted generating comparable reaction mixtures keeping limitation by

DOI: 10.1021/acs.organomet.6b00814
Organometallics XXXX, XXX, XXX–XXX

Table 2. Conditions and Results for the Polymerization of Propene with Complexes I–III in Toluene[a]

entry	complex	n[b]	p[c]	T_p[d]	T_m[e]	$mmmm$[f]	M_w[g]	$Đ$[h]	P[i]
1	I	2	3	0	165	>99	1600	2.0	4000
2	I	1	4	30	162	>99	1400	1.6	16000
3	I	1	4	50[j]	161	98	680	1.8	33000
4	I	2	4	70[j]	149	88	200	2.2	40000
5	I	5	4	90[j]	128	80	29	2.4	9500
6	I	5	4	110[j]	108	67	6	2.1	3600
7	II	2	3	0	164	>99	2200	1.5	3200
8	II	2	4	30	163	>99	1500	1.5	15000
9	II	2	4	50	162	>99	710	1.7	16000
10	II	2	4	70[j]	154	93	200	1.7	47000
11	II	5	4	90[j]	143	89	31	2.1	11000
12	II	5	4	110[j]	122	76	6	1.7	7500
13	III	2	3	0	171[l]	99.9[l]	5800[l]	1.2[l]	1000
14	III	2	4	30	170[l]	99.5[l]	1700[l]	1.5[l]	13000
15	III	2	4	50	165[l]	99.3[l]	1100[l]	1.6[l]	14000
16	III	2	4	70[j]	160[l]	98.4[l]	410[l]	1.5[l]	46000
17	III	5	4	90[k]	152	94	97	2.4	50000
18	III	5	4	110[j]	128	84	12	2.1	21000
19	I	2	3	50[j]	155	93	290	2.3	30000
20	II	2	3	50	156	97	380	1.9	19000

[a] t_p = 30 min; $V_{toluene}$ = 300 mL; scavanger (TIBA) = 2.2 mmol. [b] In micromoles. [c] $p = p_{Ar} + p_{propene}$ in bar; p_{Ar} = 1.3 bar. [d] T_p in °C ± 2 °C. [e] In °C. [f] Determined via ^{13}C NMR spectroscopy assuming the enantiomorphic site model. [g] In kg·mol^{-1}. [h] $Đ = M_w/M_n$. [i] in $kg_{PP}\cdot[mol_M\cdot(mol/L)\cdot h]^{-1}$ [j] ±5 °C. [k] ±8 °C. [l] According to ref 28.

mass-transport to a minimum or at least comparable for all three catalyst systems.

Olefin polymerization basically proceeds via π-coordination of an olefin unit followed by the migratory insertion via four-center transition state. Variation of the ligand structure of complexes **I**-**III** may affect the monomer association/dissociation equilibrium but since the rate-determining step is generally assigned to the process of olefin insertion, the focus is directed to the influence of varied ligand structure on the rate of chain propagation (ν).[40−42] The latter takes place first order with respect to the amount of added catalyst (cat) and monomer (C_3H_6), the rate constant of monomer insertion (k_P) and the fraction of catalytically active complex (χ) (eq 1).[43]

$$\nu = k_P\cdot\chi\cdot[cat]\cdot[C_3H_6] \quad (1)$$

To compare the catalytic activity of complexes **I**-**III** as a preferably unadulterated function of the chain propagation rate, the productivities are normalized to catalyst and monomer concentration (the latter determined by the equation of Busico[44]). A crucial point for the catalytically active fraction (χ) is the initial complex activation procedure being already discussed in a previous section, but also catalyst deactivation due to decomposition at high temperatures becomes progressively important thereby irreversibly lowering χ. This process is indicated by a significant drop of activity over the polymerization time excluding a prevalent impact of mass-transport limitation due to enhanced viscosity. The possible formation of resting states during the polymerization is an important as well as hardly predictable issue. Beside the interaction with aluminum alkyls being always present in the reaction mixture the role of the counterion is also essential in this connection. Whereas the applied $[B(C_6F_5)_4]^-$ anion possesses a low coordination strength to the catalytically active cationic complex in the case of $[MeB(C_6F_5)_3]^-$ the tight cation−anion interaction results in an equilibrium of active and dormant species.[45] The impact of varied ligand structure on the complex cation−anion interaction potentially affecting the coordination strength, the anion mobility, the monomer assisted dissociative displacement or the prevalent formation of solvated/outer-sphere ion pairs may depict a substantial reason for the different catalytic behavior of complexes **I**-**III**.[45,46] These interactions may directly affect the rate constant (k_P), itself representing a very complex aggregate accounting all factors of influence related to chain propagation. Most essentially, the influence of varied steric demand of the 4-aryl substituents in complexes **I**-**III** on the chain propagation step should be expressed by this constant. However, experimental determination of k_P appears to be rather difficult and is only feasible monitoring the molecular weight with respect to the reaction time. Since the reaction time to build up one polymer chain is usually well below one second only few examples of quantitative kinetic investigation are known using quenched flow techniques.[43,47−49] Consequentially, a more qualitative evaluation of the impact of varied ligand structure on the catalytic activity is in the scope of this work. The temperature dependent productivities of complexes **I**-**III** adjusted to the present complex and monomer concentration are depicted in Figure 5.

It is illustrated, that the maximum productivity of all three complexes **I**-**III** is shifted with respect to the applied polymerization temperature and the absolute value of the maximized productivity increases. Complex **I** comprising the smallest steric demand at the 4-aryl substituent, reveals its highest productivity at about 60−65 °C (~40 000 $kg_{PP}\cdot[mol_M\cdot(mol/L)\cdot h]^{-1}$). The maximum productivity is displaced up to about 70 °C (~45 000 $kg_{PP}\cdot[mol_M\cdot(mol/L)\cdot h]^{-1}$) for complex **II** and to 80−85 °C (~50 000 $kg_{PP}\cdot[mol_M\cdot(mol/L)\cdot h]^{-1}$) for the ^{t}Bu-substituted complex **III**, respectively. At low polymerization temperatures the less sterically demanding complex **I** exhibits the highest productivities leading to the assumption that chain propagation is rather limited in the case of bulkier substituted systems. Interaction of the skipping polymer chain

DOI: 10.1021/acs.organomet.6b00814
Organometallics XXXX, XXX, XXX−XXX

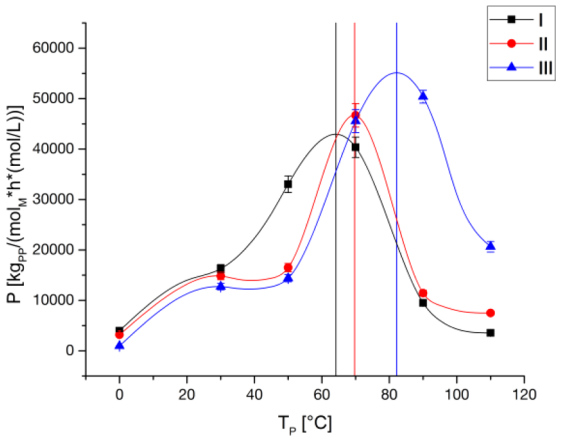

Figure 5. Spline representation of the productivity for complexes **I–III** in the polymerization of propene (see Table 2 for details). Error bars are depicted according to possible deviations during the preparation process.

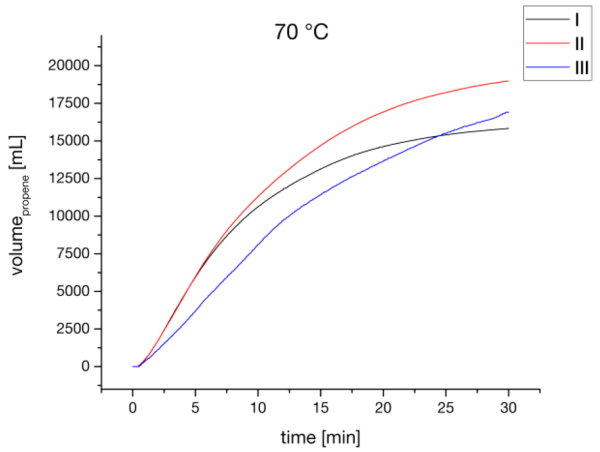

Figure 6. Consumption of propene with respect to the polymerization time at 70 °C (entries 4, 10, and 16) standardized on 2.0 μmol of **I–III**.

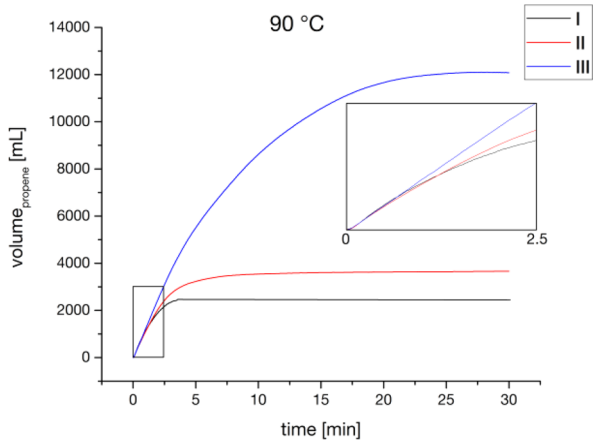

Figure 7. Consumption of propene with respect to the polymerization time at 90 °C (entries 5, 11, and 17) standardized on 2.0 μmol of **I–III**.

due to the migratory insertion mechanism with the 4-aryl substituents may exhibit a crucial role considering low rotation rates. Switching to polymerization temperatures of 30 °C results in a productivity increase of all three complexes **I-III**. Further temperature increase to 50 °C rises the productivity of **I** distinctly, whereas the more sterically encumbered complexes **II-III** need polymerization temperatures of $T_P \geq 70$ °C to become highly active. Higher steric demand from **I** to **III** in the complex framework seems to limit the catalytic activity at low to moderate temperatures. The temperature shifted progressive increase of the productivity of **I** vs **II** and **III** may be at least partially ascribed to different solubility of the produced polymer. Without going into detail on the polymer properties at this point, a more precise stereoselective behavior as well as higher molecular weights are obtained with a bulkier 4-aryl substituent. As a result, polypropylene produced at 50 °C with **I** is partly soluble, whereas that of **II** and especially **III** still precipitates thereby removing active catalyst at an early stage of the polymerization process. Consequently, **II** and **III** display high catalytic activities not until predominant solubility of the produced polymer is provided. Regarding high polymerization temperatures ($T_P \geq 70$ °C) enhanced sterical encumbrance in the complex structure accounts for higher catalytic activities. Considering the volume uptake of propene during the adopted polymerization time this observation seems to be a reason for different thermal stability of the catalytically activated complexes (Figure 6, 7).

At 70 °C the productivity, representing the averaged catalytic performance over the polymerization time, is in a comparable range for all three activated complexes **I-III**. Nevertheless, the volume uptake of propene indicates a distinct different catalytic behavior. Although complex **I** and **II** show very high initial activities (Figure 6, 70 °C, large slope of the curves), the sterically most encumbered complex **III** reveals the highest activities at longer polymerization times resulting in a similar overall volume uptake of all three catalytic systems. At 90 °C the initial activities are almost identical for all three complexes, but **III** is the only complex which is active during the whole polymerization time. By contrast, the catalytically active species of complex **I** is completely deactivated after about 4 min and **II** after about 10 min.

Polymer properties. The molecular weights are determined by the rate ratio of propagation and chain release. All three complexes **I-III** produce polymers with ultrahigh molecular weights particularly at low polymerization temperatures. Switching to higher temperatures and lower monomer concentrations endothermal elimination processes become more favored (Figure 8).

An increased steric demand of the 4-aryl substituent results in higher molecular weights of the produced polymers suggesting progressive prevention of elimination reactions. This effect is especially pronounced for **III** at lower polymerization temperatures although the lowest propagation rates of all complexes are observed under these conditions.

Crucial for the molecular weight of the polymer chains are the chain release reactions. Investigation of the olefinic end group composition facilitates the determination of chain release reactions using the catalytically activated complexes **I-III**. Due to low concentration of olefinic end groups in high molecular weight polymer samples the end group composition can only be identified in polymer samples produced at higher polymerization temperatures and lower monomer concentrations via ^{1}H NMR spectroscopy (Figure 9). In the case of complex **I** and **II** β-methyl elimination is observed as most favored chain release reaction pathway leading to the formation of allylic end groups (Figure 9, green). Vinylidene end groups as a result of β-hydride elimination can be detected as second preferred chain

DOI: 10.1021/acs.organomet.6b00814
Organometallics XXXX, XXX, XXX–XXX

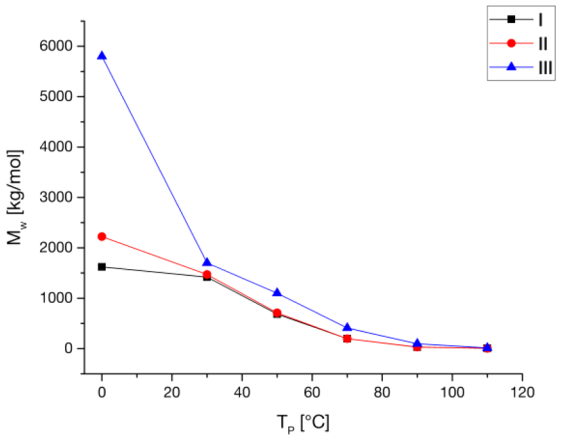

Figure 8. Weight-average molecular weight (M_w) of polypropylene dependent on the polymerization temperatures with **I**–**III** (see Table 2 for details).

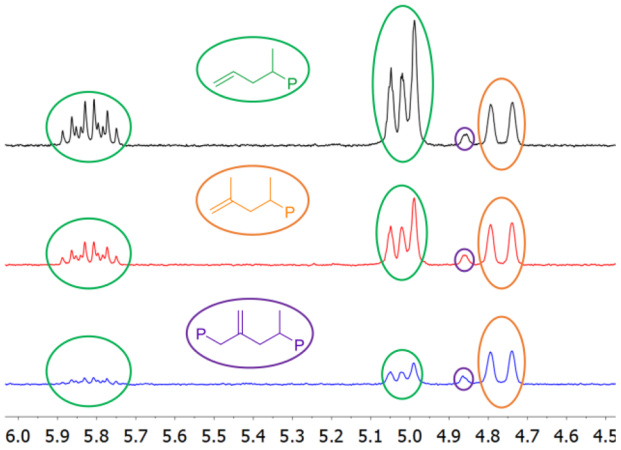

Figure 9. Determination of olefinic end group composition via ^{1}H NMR spectroscopy (at 140 °C, C_6D_5Br) of polypropylene (entries 5, 11, and 17; T_p = 90 °C) with **I** (black), **II** (red), and **III** (blue).

release reaction (Figure 9, orange). Regarding complex **III** the probability toward vinylidene end groups is higher compared to allylic end groups. Internal end groups as a result of allylic C–H bond activation are also monitored for all three complexes (Figure 9, purple).[50,51] The impact of the polymerization temperature on the selectivity of β-hydride and β-methyl elimination is depicted in Figure 10 considering the polymerization results at 110 °C.

At 90 °C as well as 110 °C the catalytically active species of complex **I** bearing the lowest steric demand at the 4-aryl substituent possesses the highest selectivity toward allylic chain ends. This fact contradicts with previous studies revealing much higher selectivities toward β-methyl transfer in the case of the bulkier substituted $Cp^*_2HfCl_2$/MAO system (M: Zr, Hf) compared to the unsubstituted Cp_2HfCl_2/MAO system (M: Zr, Hf).[52−55] Rising the polymerization temperature favors the pathway of β-methyl elimination in all three cases. Varying the temperature from 90 to 110 °C particularly affects the end group selectivity of complex **III** resulting in the predominant formation of allylic chain ends at 110 °C in contrast to the observed end group composition at 90 °C.

In accordance to Figure 8 the average molecular weight decreases with elevated temperatures since all chain release reactions more preferentially occur. The results of Figure 10

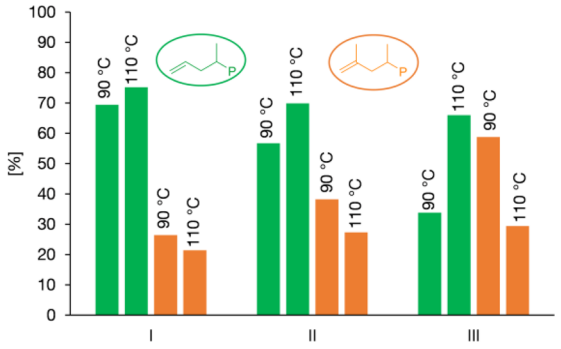

Figure 10. Determination of allylic and vinylidene chain ends of polypropylene produced at 90 and 110 °C (entries 5, 6, 11, 12, 17, and 18).

suggest that especially β-methyl elimination is accelerated rising the temperature. This is in line with a higher estimated activation barrier for the process of β-methyl compared to β-hydride elimination considering the notable energy difference for C–C vs C–H bond cleavage.[56] An increased steric demand of the 4-aryl substituents prevents both elimination pathways, whereupon the process of β-methyl elimination is obviously reduced more distinctly.

For ^{i}PP produced by complex **III** very low amounts of regiodeffects are reported.[28] The results of **I** and **II** confirm the concise regioselectivity for these type of complexes since neither 2,1-erythro nor 3,1-isomerization regio deffects are detected using standard ^{13}C NMR spectroscopy (s. Experimental). The remarkable selectivities especially at elevated polymerization temperatures may be attributed to the high rigidity in all three catalytic systems. The rigidity preserves the accurate molecular structure being indispensible for a presice regio control mechanism in conditions usually stimulating potentially undesired rotational, vibrational and motional processes.

All three complexes exhibit almost perfect stereoselective behavior in the polymerization of propene at low temperatures following the mechanism of enantiomorphic site control.[57−60] Switching to higher polymerization temperatures as well as lower monomer concentrations isolated stereoerrors become detectable. The tacticity is determined by the ratio of the *mmmm*-pentad to the sum of all pentads (Figure 11).

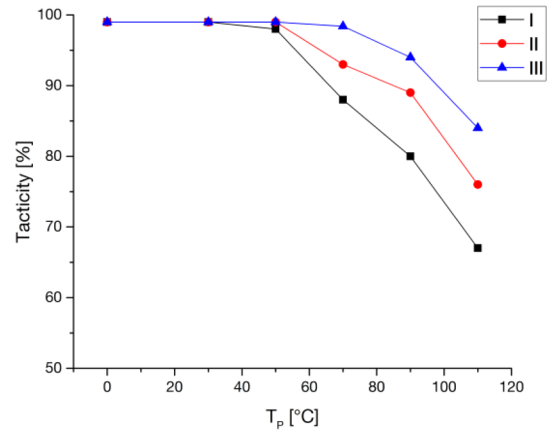

Figure 11. Tacticities (% *mmmm*) of the polymers produced with complexes **I**–**III** determined via ^{13}C NMR spectroscopy (see Table 2 for details).

DOI: 10.1021/acs.organomet.6b00814
Organometallics XXXX, XXX, XXX–XXX

Assignment of the isotacticity (% *mmmm*) via ^{13}C NMR spectroscopy indicates at least 99% *mmmm* regarding polymerization temperatures up to 30 °C for **I** and **II** with respect to the signal-to-noise ratio, although no other pentads are observable. All tacticities of polymers produced with complex **III** (except entry 17 + 18) were determined with an accuracy of ±0.1%.[28] Investigation of the pentad distribution at polymerization temperatures above 50 °C reveals the presence of additional pentads (*mmmr*, *mmrr*, *mrrm*) attributed to isolated stereo errors.

Taking into consideration that the polymerizations between 70−110 °C were performed at isobar pressure, lower monomer concentrations at higher temperatures evoke predominant impact on the stereo control mechanism beside the general loss of selectivity caused by rising the temperature itself. Particularly stereoerror formation via chain end epimerization[61] is favored at low monomer concentration and is attributed to be the main reason turning down the isotacticity employing complex **I-III** under these conditions.[44,62−65] This assumption is supported by polymers produced with **I** and **II** at 50 °C and 3 bar, possessing significantly lower tacticities (**I**: 93% *mmmm*, **II**: 97% *mmmm*) than the ones produced at 4 bar. Consequently, complex **III** comprising the highest steric demand at the 4-aryl substituent is able to preserve the formation of isotactic sequences at elevated temperatures best, whereas **I** produces polymers with the lowest amount of *mmmm*-pentads. These results indicate that an increased steric demand more sufficiently prevents the cascade process of chain end epimerization comparing complex **I-III**. Disregarding the predominant stereoerror formation via chain end epimerization in the presence of low monomer concentration, we believe, that the enantiofacial selectivity of our systems is still accurate at elevated temperatures due to the high rigidity of the complexes. One example demonstrating the precise catalytic control at higher temperatures is the polymerization with **III** at 70 °C increasing the monomer concentration from 0.88 M (Entry 16) to 1.53 M. The result is a highly isoselective polymer with an *mmmm*-pentad distribution of 99.0%.[28]

The melting behavior of the polymers is mainly influenced by the tacticity of the polypropylenes. In the case of short chain lengths the average molecular weight possesses a more distinguished impact on the melting transition.[66] The melting transition of all generated polymers is depicted in Figure 12.

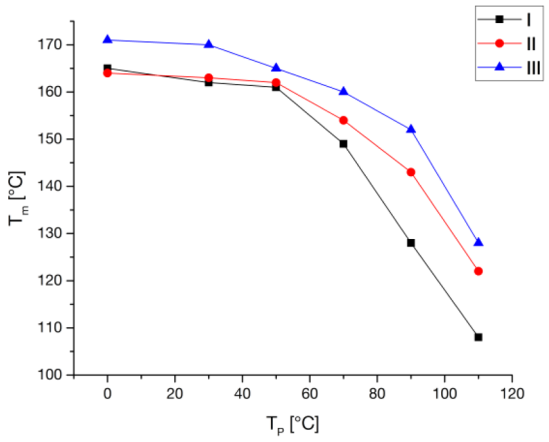

Figure 12. Melting transition of polypropylene samples produced at different polymerization temperatures with **I−III** (see Table 2 for details).

High melting temperatures above 160 °C are observed for polymerization temperatures up to 50 °C in all cases. An overall decrease of the melting transitions is noticed for the polymers of complexes **I-III** applying higher polymerization temperatures, at which the effect is less pronounced with increased steric demand of the ligand. The results are in line with the determined tacticities (Figure 11) as well as molecular weights (Figure 8).

Regarding industrial application, the focus is directed to highly productive catalyst systems, most substantially, comprising long-term stability. A precise stereo- and regio control mechanism in combination with high molecular weight polymer chains are indispensable to ensure the quality of the produced high performance polyolefins. Considering the production process, elevated temperatures are always preferred to improve heat transmission (larger ΔT) as well as the processability, since better solubility of the produced polymer is assured. In this context, the most promising results are obtained with the catalytic system **III** revealing the highest selectivities and productivities combined with the most distinctive temperature stability. The high rigidity in the complex framework, provided by the combined steric effects of the 7-OMe and the sterically encumbered 4-[(3′,5′-*tert*-butyl)-phenyl] substituents, is suggested to be key for this essential contribution. The introduced rigidity-concept as a result of the unique substitution pattern displays a new, alternative approach for further catalyst design and development.

CONCLUSION

In this report two novel C_2-symmetric indenyl based *ansa*-hafnocene complexes with 4-aryl substituents of varied steric demand (**I-II**) were synthesized enabling a comparative study with the literature known complex (**III**). The latter is stated as benchmark for the catalysis of high melting ultrahigh molecular weight ^{i}PP comprising extraordinary precise stereo- and regioregularity. Complete characterization including X-ray diffraction analysis was conducted for both new complexes illustrating the crucial impact of the 4-aryl substituent on the coordination gap aperture. The activated complexes **I-III** were examined regarding their polymerization behavior applying identical conditions. The varied steric demand of the 4-aryl substituent revealed considerable impact on the maximum productivity with respect to the polymerization temperature. Therefore, the direct relationship between complex structure and catalytic activity is extensively discussed with respect to the combined impact of activation, monomer diffusion rate, catalyst deactivation and rate of chain growth. The highest temperatures to reach the maximized productivity in combination with the largest overall catalytic activity were necessary for the most sterically encumbered complex **III**. GPC analysis determined remarkable high molecular weights for the polymers of all three complexes at low polymerization temperatures. A decrease of the average molecular weight is observed applying higher polymerization temperatures as well as lower monomer concentrations. Increased steric encumbrance of the ligand leads to higher molecular weights due to enhanced prevention of chain release reactions. Olefinic end group analysis discloses increased selectivity toward allylic vs vinylidene end groups regarding elevated polymerization temperatures, since β-methyl elimination is rather accelerated. Furthermore, the process of the β-methyl elimination is particularly prevented in the case of increased steric demand at the 4-aryl substituent. At low to moderate polymerization temperatures going along with higher

DOI: 10.1021/acs.organomet.6b00814
Organometallics XXXX, XXX, XXX−XXX

monomer concentrations the catalytic performance in terms of stereoregularity is very concise for all three complexes **I**-**III**. Consequentially, the *mmmm*-pentad is exclusively detected using ^{13}C NMR spectroscopy. The formation of isolated stereoerrors, predominant a result of chain end epimerization, rather occurs at lower monomer concentrations. The sterically most encumbered complex **III** is capable of still preserving the highest isotacticities impeding the cascade reaction of chain end epimerization better than **I** and **II**. Accurate regioselecitivties for all polymers produced with **I**-**III** were detected in a broad temperature range. High rigidity in the complex framework is key for a precise stereo and regio control up to elevated temperatures. DSC analysis provides a high melting behavior for the polymer of all three complexes dependent on the varied polymerization conditions in analogy to the determined tacticities and molecular weights.

EXPERIMENTAL SECTION

General. All reactions containing air- and moisture-sensitive compounds were performed under argon atmosphere using standard Schlenk or glovebox techniques. All chemicals, unless otherwise stated, were purchased from Aldrich, Acros, or VWR and used as received. Dry toluene and *n*-pentane were obtained from an MBraun MB-SPS-800 solvent purification system. Deuterated dichloromethane was refluxed over CaH_2 and distilled prior to use. Propene (99.5% by Westfalen AG) was purified by passage through two columns filled with BASF catalyst (R3-11) and molecular sieves 3−4 Å. Elemental analysis was conducted with a EURO EA (HEKA tech) instrument equipped with a CHNS combustion analyzer.

^1H and ^{13}C NMR measurements were recorded on a Bruker ARX-300, AV-500C, AV400, or AV500 spectrometer at ambient temperature. Chemical shifts δ are reported in ppm relative to tetramethylsilane and calibrated to the residual ^1H or ^{13}C signal of the deuterated solvent. Polymer spectra were measured with an ARX-300 spectrometer at 140 °C in bromobenzene-d_5 with 50−60 mg/mL.

Gel permeation chromatography (GPC) was performed with a PL-GPC 220 instrument equipped with 2× Olexis 300 mm × 7.5 mm columns and triple detection via differential refractive index detector, PL-BV 400 HT viscometer, and light scattering (Precision Detectors model 2040; 15°, 90°). Measurements were performed at 160 °C using 1,2,4-trichlorobenzene (TCB; 30 mg BHT/L) with a constant flow rate of 1 mL/min and a calibration set with narrow MWD polystyrene (PS) and polyethylene (PE) standards. Samples were prepared dissolving 0.9−1.1 mg of polymer in 1.0 mL of stabilized TCB for 10−15 min at 160 °C immediately before each measurement.

Differential scanning calorimetry (DSC) analysis was conducted on a DSC Q2000 instrument. Polymer (3−8 mg) was sealed into a DSC aluminum pan and heated from 20 to 200 °C at 10 °C/min. After holding the temperature for 2 min, the sample was cooled down to 20 °C at 10 °C/min and heated up again in the same manner. The reported values are those determined in the second heating cycle.

Synthesis. All compounds that are not listed below were synthesized according to literature procedures.[28,67,68]

Bis(4-bromo-7-methoxy-2-methylindenyl)dimethyl Silane, ***2.*** 4-Bromo-7-methoxy-2-methylindene (10.3 g, 43.1 mmol, 2.00 equiv) was diluted in 200 mL of dry toluene/dioxane (1/1) in a pressurizable Schlenk flask. At −10 °C, 17.2 mL (43.1 mmol 2.00 equiv) of ^{n}BuLi, 2.5 M in hexane, was added dropwise to the solution. After stirring at room temperature for 2 h, 2.62 mL (21.5 mmol, 1.00 equiv) of dichlorodimethylsilane was added at −10 °C. After stirring at 60 °C for additional 24 h, the reaction mixture was poured into 50 mL of water. Diethyl ether (150 mL) was added, phases were separated, and the organic layer was washed with water (150 mL) and brine (150 mL). The organic phase was dried with Na_2SO_4, the solvent is evaporated, and the crude product was recrystallized in a DCM/MeOH mixture leading to 8.25 g (72%) of colorless needles (**2**). Anal. Calcd for $C_{24}H_{26}Br_2O_2Si$: C, 53.95; H, 4.90. Found: C, 53.99; H, 4.78. ^1H NMR (500 MHz, $CDCl_3$, 298 K): δ (ppm) = 7.28 (d, ^3J = 8.5 Hz, 2H, H−Ar), 6.60 (m, 2H, −CH═), 6.53 (d, ^3J = 8.5 Hz, 2H, H−Ar), 4.24 (s, 2H, −CH−Si), 3.85 (s, 6H, $-OCH_3$), 2.24 (d, ^3J = 1.4 Hz, 6H, $-CH_3$), −0.44 (s, 6H, Si−CH_3). ^{13}C NMR (126 MHz, $CDCl_3$ 298 K): δ (ppm) = 153.51, 150.19, 145.96, 134.30, 129.05, 125.54, 106.65, 105.62, 54.99, 48.18, 17.70, −3.71.

7-(3′,5′-Dimethylphenyl)-4-methoxy-2-methylindene, ***3a.*** All solvents were degassed prior to use. A solution of 4.63 g (30.8 mmol, 1.10 equiv) of (3,5-dimethylphenyl)boronic acid in ethanol (40 mL) and a solution of 3.88 g (3.36 mmol, 0.12 equiv) $Pd(PPh_3)_4$ in toluene (200 mL) were added to 6.70 g (28.0 mmol, 1.00 equiv) of 4-bromo-7-methoxy-2-methylindene. After the subsequent addition of 56.0 mL (56.0 mmol, 2.00 equiv) of 1 M NaOH solution, the mixture was refluxed for 3 days. Water (250 mL) and toluene (250 mL) were added, phases were separated, and the aqueous phase was extracted two times with toluene (2 × 100 mL). The combined organic layers were dried over Na_2SO_4, and the solvent was removed *in vacuo*. Compound **3a** was isolated via column chromatography (toluene, R_f = 0.75) as a white solid (6.10 g, 82%). Anal. Calcd for $C_{19}H_{20}O$: C, 86.32; H, 7.63. Found: C, 86.69; H, 7.60. ^1H NMR (300 MHz, $CDCl_3$, 298 K): δ (ppm) = 7.11 (s, 2H, H−Ar′), 7.07 (d, ^3J = 8.3 Hz, 1H, H−Ar), 6.97 (s, 1H, H−Ar′), 6.84 (d, ^3J = 8.3 Hz, 1H, H−Ar), 6.64 (s, 1H, −CH═), 3.88 (s, 3H, $-OCH_3$), 3.39 (s, 2H, $-CH_2-$), 2.35 (s, 6H, CH_3−Ar′), 2.13 (s, 3H, $-CH_3$). ^{13}C NMR (75 MHz, $CDCl_3$ 298 K): δ (ppm) = 152.05, 145.28, 143.04, 141.52, 138.40, 134.95, 131.42, 128.72, 126.66, 125.76, 123.46, 109.66, 55.97, 43.96, 21.68, 16.93.

Bis[4-phenyl-7-methoxy-2-methylindenyl)]dimethyl Silane, ***4.*** All solvents were degassed prior to use. A solution of 6.10 g (50.0 mmol, 4.00 equiv) of phenylboronic acid in ethanol (70 mL) as well as a solution of 3.46 g (2.99 mmol, 0.24 equiv) of $Pd(PPh_3)_4$ in toluene (400 mL) were added to 6.66 g (12.5 mmol, 1.00 equiv) of bis(4-bromo-7-methoxy-2-methylindenyl)dimethyl silane (**2**). After the subsequent addition of 50.0 mL (50.0 mmol, 4.00 equiv) of 1 M NaOH solution, the mixture was refluxed for 3 days. Water (200 mL) and toluene (200 mL) were added, phases were separated, and the aqueous phase was extracted two times with toluene (2 × 100 mL). The combined organic layers were dried over Na_2SO_4, and the solvent was removed *in vacuo*. A 1:1 mixture of *rac*-/*meso*-isomers (**4**) was obtained via column chromatography (pentane/EtOAc 20/1, R_f = 0.36). Recrystallization in DCM/MeOH led to the desired product as colorless needles (5.20 g, 79%). Anal. Calcd for $C_{36}H_{36}O_2Si$ × 1/3 CH_2Cl_2: C, 78.34; H, 6.63. Found: C, 78.26; H, 6.60 (presence of additional CH_2Cl_2 was confirmed via NMR spectroscopy). ^1H NMR (300 MHz, $CDCl_3$, 298 K): δ (ppm) = 7.54 (m, 4H, H−Ar′), 7.45 (m, 4H, H−Ar′), 7.33 (m, 2H, H−Ar′), 7.24 (dd, ^3J = 8.2, 1.7 Hz, 2H, H−Ar), 6.74 (m, 4H, H−Ar, −CH═), 4.23, 4.06 (s, 2H, −CH−Si), 3.92, 3.85 (s, 6H, $-OCH_3$), 2.30, 2.17 (s, 6H, $-CH_3$), −0.20, −0.22, −0.34 (s, 6H, Si−CH_3). ^{13}C NMR (75 MHz, $CDCl_3$ 298 K): δ (ppm) = 153.70, 153.66, 149.82, 149.63, 144.35, 144.26, 141.42, 133.48, 128.97, 128.95, 128.43, 127.75, 127.68, 126.78, 126.77, 126.34, 125.19, 125.08, 105.41, 105.35, 54.78, 54.67, 47.06, 46.62, 17.81, 17.72, −2.65, −3.83, −3.85.

Bis[4-(3′,5′-dimethylphenyl)-7-methoxy-2-methylindenyl)]-dimethyl Silane, ***5a.*** Compound **3a** (5.97 g, 22.6 mmol, 2.00 equiv) was diluted in 100 mL of dry toluene/dioxane (1/1) in a pressurizable Schlenk flask. At −10 °C, 6.42 mL (22.6 mmol 2.00 equiv) of ^{n}BuLi, 2.4 M in hexane, was added dropwise to the solution. After stirring at room temperature for 2 h, 1.38 mL (11.3 mmol, 1.00 equiv) of dichlorodimethylsilane was added at −10 °C. After stirring at 60 °C for additional 24 h, the reaction mixture was poured into 25 mL of water. Diethyl ether (100 mL) was added, phases were separated, and the organic layer was washed with water (70 mL) and brine (70 mL). The organic phase was dried with Na_2SO_4, the solvent was evaporated, and the crude product was recrystallized in a DCM/MeOH mixture leading to 3.11 g (47%) of a 1:1 *rac*-/*meso*-isomer mixture as white solid. Anal. Calcd for $C_{40}H_{44}O_2Si$: C, 82.14; H, 7.58. Found: C, 81.79; H, 7.53. ^1H NMR (300 MHz, $CDCl_3$, 298 K): δ (ppm) = 7.19, 7.18 (d, ^3J = 8.3 Hz, 2H, H−Ar), 7.12, 7.10 (s, 4H, H−Ar′), 6.96 (s, 2H, H−Ar′), 6.71 (m, 4H, H−Ar, −CH═), 4.22, 4.02 (s, 2H, −CH−Si), 3.90, 3.84 (s, 6H, $-OCH_3$), 2.39, 2.36 (s, 12H, CH_3−Ar′), 2.28, 2.15 (s, 6H, $-CH_3$), −0.23, −0.25, −0.39 (s, 6H, Si−CH_3). ^{13}C NMR (75

DOI: 10.1021/acs.organomet.6b00814
Organometallics XXXX, XXX, XXX−XXX

MHz, $CDCl_3$ 298 K): δ (ppm) = 153.62, 153.59, 149.57, 149.39, 144.38, 144.29, 141.43, 137.87, 137.86, 133.51, 133.43, 128.05, 127.99, 127.92, 126.87, 126.85, 126.78, 126.74, 125.34, 125.20, 105.35, 105.28, 54.78, 54.65, 47.12, 46.61, 21.60, 17.81, 17.74, −2.57, −3.76, −3.79.

rac-Dimethylsilanediylbis(4-phenyl-7-methoxy-2-methylindenyl)-hafnium Dichloride, I. Compound **4** (750 mg, 1.42 mmol, 1.00 equiv) was dissolved in 50 mL of dry toluene and cooled down to −78 °C, and 1.67 mL (2.84 mmol, 2.00 equiv) of 1.7 M ^{t}BuLi solution in pentane was added dropwise. After maintaining the temperature for 1 h, the reaction mixture was stirred for additional 3 h at room temperature. The yellow suspension was cooled down to 0 °C and subsequently transferred via cannula to a suspension of 454 mg (1.42 mmol, 1.00 equiv) of $HfCl_4$ in 25 mL of dry toluene at −78 °C. The reaction mixture was allowed to thaw overnight resulting in an orange suspension. The suspension was filtered, and the residue was extracted with dry toluene (2 × 100 mL). The extract was concentrated to 10 mL and cooled down to −20 °C overnight. Pure *rac*-isomer (110 mg, 10%) was obtained as an orange crystalline solid after removal of the overlaying solution. Anal. Calcd for $C_{36}H_{34}Cl_2HfO_2Si$: C, 55.71; H, 4.42. Found: C, 55.52; H, 4.32. ^{1}H NMR (400 MHz, $C_2D_2Cl_2$, 298 K): δ (ppm) = 7.60 (m, 4H, H−Ar′), 7.41 (m, 4H, H−Ar′, H−Ar), 7.31 (m, 4H, H−Ar′), 6.86 (s, 2H, −CH═), 6.43 (d, ^3J = 7.8 Hz, 2H, H−Ar), 3.92 (s, 6H, $-OCH_3$), 2.24 (s, 6H, $-CH_3$), 1.21 (s, 6H, Si$-CH_3$). ^{13}C NMR (100 MHz, $C_2D_2Cl_2$, 298 K): δ (ppm) = 156.11, 140.40, 133.16, 132.93, 130.63, 129.07, 129.01, 128.26, 127.60, 121.71, 120.33, 103.26, 85.70, 17.67, 6.17.

rac-Dimethylsilanediylbis[4-(3′,5′-dimethylphenyl)-7-methoxy-2-methylindenyl)]hafnium Dichloride, II. Compound **5a** (1.33 g, 2.27 mmol, 1.00 equiv) was dissolved in 70 mL of dry toluene and cooled down to −78 °C, and 2.68 mL (4.55 mmol, 2.00 equiv) of 1.7 M ^{t}BuLi solution in pentane was added dropwise. After maintaining the temperature for 1 h, the reaction mixture was stirred for additional 3 h at room temperature. The yellow suspension was cooled down to 0 °C and subsequently transferred via cannula to a suspension of 727 mg (2.27 mmol, 1.00 equiv) of $HfCl_4$ in 40 mL of dry toluene at −78 °C. The reaction mixture was allowed to thaw overnight resulting in a dark yellow suspension. After filtration, the solvent of the filtrate was distilled off, and the residue was washed with dry pentane (2 × 100 mL) and a 1:2 toluene/pentane-mixture (240 mL). After recrystallization in a toluene/pentane mixture, 360 mg (19%) of yellow powder was obtained containing the pure *rac*-isomer. Anal. Calcd for $C_{40}H_{42}Cl_2HfO_2Si$: C, 57.73; H, 5.09. Found: C, 57.69; H, 4.95. ^{1}H NMR (400 MHz, CD_2Cl_2, 298 K): δ (ppm) = 7.26 (d, ^3J = 7.8 Hz, 2H, H−Ar), 7.24 (s, 4H, H−Ar′), 6.96 (s, 2H, −CH═), 6.87 (s, 2H, H−Ar′), 6.40 (d, ^3J = 7.8 Hz, 2H, H−Ar), 3.91 (s, 6H, $-OCH_3$), 2.31 (s, 12H, CH_3-Ar′), 2.25 (s, 6H, $-CH_3$), 1.20 (s, 6H, Si$-CH_3$). ^{13}C NMR (100 MHz, CD_2Cl_2 298 K): δ (ppm) = 155.96, 140.10, 138.58, 133.07, 132.83, 130.93, 129.20, 127.85, 126.81, 122.12, 120.29, 103.20, 85.45, 21.62, 17.66, 6.16.

Polymerization. All polymerization reactions were performed in a 1.1 L Büchi steel autoclave equipped with a paddle agitator, temperature sensor, and heating/cooling jacket attached to a cryo-/thermostat unit (Thermo Scientific HAAKE DynaMax). Ar-pressure for all manipulations was set at 1.3 bar. Prior to polymerization, the autoclave was equipped with 300 mL of dry toluene and 2.0 mL of 1.1 M TIBA solution in toluene and heated up to 90 °C. After maintaining the temperature for 15 min, the scrubbing solution was released. For the polymerization, the autoclave was charged with 280 mL of dry toluene and 2.0 mL of 1.1 M TIBA solution in toluene. The metallocene complex (1.0 equiv) was dissolved in 10 mL of toluene and preactivated with 200 equiv of TIBA at 60 °C for 1 h. After the desired temperature was adjusted, the activated metallocene solution was transferred into the autoclave and was pressurized with propene. When the system was equilibrated and stable, the polymerization was started adding 5.0 equiv of $[Ph_3C][B(C_6F_5)_4]$ dissolved in 10 mL of toluene to the autoclave via a pressure buret (p_{pol} + 1.0 bar). The propene consumption was monitored using a gas flow meter (Bronkhorst F-111C-HA-33P). Temperature, pressure, time, and total propene consumption were recorded as well. The polymerization reaction was quenched with 2.0 mL of methanol, and the reaction mixture was poured into 1.0 L of acidified methanol. Precipitated polymer was removed from the autoclave, and all combined polymer was washed exhaustively and dried at 70 °C *in vacuo* overnight.

■ ASSOCIATED CONTENT

Supporting Information

The Supporting Information is available free of charge on the ACS Publications website at DOI: 10.1021/acs.organomet.6b00814.

^{1}H NMR and ^{13}C NMR spectra of the new key compounds **I** and **II**, UV VIS spectra, ^{1}H NMR spectra for end group analysis, ^{13}C NMR spectra for tacticity determination, charts providing propene consumption during the polymerization time, SC-XRD data (PDF)

Crystallographic information for compounds **I** and **II** (CIF)

■ AUTHOR INFORMATION

Corresponding Author

*E-mail: rieger@tum.de. Tel: +49-89-289-13570. Fax: +49-89-289-13562.

ORCID

Bernhard Rieger: 0000-0002-0023-884X

Notes

The authors declare no competing financial interest.

■ ACKNOWLEDGMENTS

The authors thank Philipp Pahl and Daniel Wendel for proofreading the manuscript and valuable discussions. The second author D. L. substantially contributed to this work during his time as a co-worker of the Wacker-Lehrstuhl für Makromolekulare Chemie.

■ REFERENCES

(1) Kaminsky, W.; Külper, K.; Brintzinger, H. H.; Wild, F. R. W. P. *Angew. Chem., Int. Ed. Engl.* **1985**, *24*, 507−508.

(2) Kaminsky, W. *Macromolecules* **2012**, *45*, 3289−3297.

(3) Wild, F. R. W. P.; Zsolnai, L.; Huttner, G.; Brintzinger, H. H. *J. Organomet. Chem.* **1982**, *232*, 233−247.

(4) Resconi, L.; Cavallo, L.; Fait, A.; Piemontesi, F. *Chem. Rev.* **2000**, *100*, 1253−1345.

(5) Ewen, J. A. *J. Am. Chem. Soc.* **1984**, *106*, 6355−6364.

(6) Ziegler, K.; Holzkamp, E.; Breil, H.; Martin, H. *Angew. Chem.* **1955**, *67*, 541−547.

(7) Natta, G. *Angew. Chem.* **1956**, *68*, 393−403.

(8) Coates, G. W.; Waymouth, R. M. *Science* **1995**, *267*, 217−219.

(9) Mallin, D. T.; Rausch, M. D.; Lin, Y. G.; Dong, S.; Chien, J. C. W. *J. Am. Chem. Soc.* **1990**, *112*, 2030−2031.

(10) Dietrich, U.; Hackmann, M.; Rieger, B.; Klinga, M.; Leskelä, M. *J. Am. Chem. Soc.* **1999**, *121*, 4348−4355.

(11) Cobzaru, C.; Hild, S.; Boger, A.; Troll, C.; Rieger, B. *Coord. Chem. Rev.* **2006**, *250*, 189−211.

(12) Spaleck, W.; Antberg, M.; Rohrmann, J.; Winter, A.; Bachmann, B.; Kiprof, P.; Behm, J.; Herrmann, W. A. *Angew. Chem., Int. Ed. Engl.* **1992**, *31*, 1347−1350.

(13) Spaleck, W.; Kueber, F.; Winter, A.; Rohrmann, J.; Bachmann, B.; Antberg, M.; Dolle, V.; Paulus, E. F. *Organometallics* **1994**, *13*, 954−963.

(14) Ewen, J. A.; Zambelli, A.; Longo, P.; Sullivan, J. M. *Macromol. Rapid Commun.* **1998**, *19*, 71−73.

(15) Stehling, U.; Diebold, J.; Kirsten, R.; Roell, W.; Brintzinger, H. H.; Juengling, S.; Muelhaupt, R.; Langhauser, F. *Organometallics* **1994**, *13*, 964−970.

DOI: 10.1021/acs.organomet.6b00814
Organometallics XXXX, XXX, XXX−XXX

(16) Kuklin, M. S.; Virkkunen, V.; Castro, P. M.; Izmer, V. V.; Kononovich, D. S.; Voskoboynikov, A. Z.; Linnolahti, M. *J. Mol. Catal. A: Chem.* **2016**, *412*, 39−46.
(17) Panchenko, V. N.; Babushkin, D. E.; Brintzinger, H. H. *Macromol. Rapid Commun.* **2015**, *36*, 249−253.
(18) Press, K.; Cohen, A.; Goldberg, I.; Venditto, V.; Mazzeo, M.; Kol, M. *Angew. Chem., Int. Ed.* **2011**, *50*, 3529−3532.
(19) Razavi, A.; Thewalt, U. *Coord. Chem. Rev.* **2006**, *250*, 155−169.
(20) Kirillov, E.; Marquet, N.; Razavi, A.; Belia, V.; Hampel, F.; Roisnel, T.; Gladysz, J. A.; Carpentier, J.-F. *Organometallics* **2010**, *29*, 5073−5082.
(21) Kirillov, E.; Marquet, N.; Bader, M.; Razavi, A.; Belia, V.; Hampel, F.; Roisnel, T.; Gladysz, J. A.; Carpentier, J.-F. *Organometallics* **2011**, *30*, 263−272.
(22) Bader, M.; Marquet, N.; Kirillov, E.; Roisnel, T.; Razavi, A.; Lhost, O.; Carpentier, J.-F. *Organometallics* **2012**, *31*, 8375−8387.
(23) Kiesewetter, E. T.; Randoll, S.; Radlauer, M.; Waymouth, R. M. *J. Am. Chem. Soc.* **2010**, *132*, 5566−5567.
(24) Bochmann, M. *Organometallics* **2010**, *29*, 4711−4740.
(25) Chen, E. Y.-X.; Marks, T. J. *Chem. Rev.* **2000**, *100*, 1391−1434.
(26) Bryliakov, K. P.; Talsi, E. P.; Voskoboynikov, A. Z.; Lancaster, S. J.; Bochmann, M. *Organometallics* **2008**, *27*, 6333−6342.
(27) Alt, H. G.; Köppl, A. *Chem. Rev.* **2000**, *100*, 1205−1222.
(28) Schöbel, A.; Herdtweck, E.; Parkinson, M.; Rieger, B. *Chem. - Eur. J.* **2012**, *18*, 4129−4129.
(29) Tranchida, D.; Mileva, D.; Resconi, L.; Rieger, B.; Schöbel, A. *Macromol. Chem. Phys.* **2015**, *216*, 2171−2178.
(30) Theurkauff, G.; Bader, M.; Marquet, N.; Bondon, A.; Roisnel, T.; Guegan, J.-P.; Amar, A.; Boucekkine, A.; Carpentier, J.-F.; Kirillov, E. *Organometallics* **2016**, *35*, 258−276.
(31) Song, F.; Cannon, R. D.; Lancaster, S. J.; Bochmann, M. *J. Mol. Catal. A: Chem.* **2004**, *218*, 21−28.
(32) Kuklin, M. S.; Virkkunen, V.; Castro, P. M.; Resconi, L.; Linnolahti, M. *Eur. J. Inorg. Chem.* **2015**, *2015*, 4420−4428.
(33) Izmer, V. V.; Lebedev, A. Y.; Nikulin, M. V.; Ryabov, A. N.; Asachenko, A. F.; Lygin, A. V.; Sorokin, D. A.; Voskoboynikov, A. Z. *Organometallics* **2006**, *25*, 1217−1229.
(34) Shaltout, R. M.; Corey, J. Y.; Rath, N. P. *J. Organomet. Chem.* **1995**, *503*, 205−212.
(35) Moehring, P. C.; Coville, N. J. *Coord. Chem. Rev.* **2006**, *250*, 18−35.
(36) Brintzinger, H. H.; Fischer, D.; Mülhaupt, R.; Rieger, B.; Waymouth, R. M. *Angew. Chem., Int. Ed. Engl.* **1995**, *34*, 1143−1170.
(37) Schulte, J.; Sell, T.; Thorn, M. G.; Winter, A.; Dimeska, A. International Patent WO2009054831A1, 2009.
(38) Bochmann, M.; Lancaster, S. J. *Angew. Chem., Int. Ed. Engl.* **1994**, *33*, 1634−1637.
(39) Zhou, J.; Lancaster, S. J.; Walker, D. A.; Beck, S.; Thornton-Pett, M.; Bochmann, M. *J. Am. Chem. Soc.* **2001**, *123*, 223−237.
(40) Laine, A.; Linnolahti, M.; Pakkanen, T. A.; Severn, J. R.; Kokko, E.; Pakkanen, A. *Organometallics* **2010**, *29*, 1541−1550.
(41) Laine, A.; Linnolahti, M.; Pakkanen, T. A.; Severn, J. R.; Kokko, E.; Pakkanen, A. *Organometallics* **2011**, *30*, 1350−1358.
(42) Ehm, C.; Budzelaar, P. H. M.; Busico, V. *J. Organomet. Chem.* **2015**, *775*, 39−49.
(43) Cipullo, R.; Melone, P.; Yu, Y.; Iannone, D.; Busico, V. *Dalton Transactions* **2015**, *44*, 12304−12311.
(44) Busico, V.; Brita, D.; Caporaso, L.; Cipullo, R.; Vacatello, M. *Macromolecules* **1997**, *30*, 3971−3977.
(45) Bochmann, M. *J. Organomet. Chem.* **2004**, *689*, 3982−3998.
(46) Song, F.; Lancaster, S. J.; Cannon, R. D.; Schormann, M.; Humphrey, S. M.; Zuccaccia, C.; Macchioni, A.; Bochmann, M. *Organometallics* **2005**, *24*, 1315−1328.
(47) Ciancaleoni, G.; Fraldi, N.; Budzelaar, P. H. M.; Busico, V.; Cipullo, R.; Macchioni, A. *J. Am. Chem. Soc.* **2010**, *132*, 13651−13653.
(48) Ehm, C.; Cipullo, R.; Budzelaar, P. H. M.; Busico, V. *Dalton Transactions* **2016**, *45*, 6847−6855.
(49) Song, F.; Cannon, R. D.; Bochmann, M. *J. Am. Chem. Soc.* **2003**, *125*, 7641−7653.
(50) Resconi, L.; Camurati, I.; Sudmeijer, O. *Top. Catal.* **1999**, *7*, 145−163.
(51) Resconi, L. *J. Mol. Catal. A: Chem.* **1999**, *146*, 167−178.
(52) Resconi, L.; Piemontesi, F.; Franciscono, G.; Abis, L.; Fiorani, T. *J. Am. Chem. Soc.* **1992**, *114*, 1025−1032.
(53) Yang, P.; Baird, M. C. *Organometallics* **2005**, *24*, 6005−6012.
(54) Yang, P.; Baird, M. C. *Organometallics* **2005**, *24*, 6013−6018.
(55) Suzuki, Y.; Yasumoto, T.; Mashima, K.; Okuda, J. *J. Am. Chem. Soc.* **2006**, *128*, 13017−13025.
(56) Sini, G.; Macgregor, S. A.; Eisenstein, O.; Teuben, J. H. *Organometallics* **1994**, *13*, 1049−1051.
(57) Castonguay, L. A.; Rappe, A. K. *J. Am. Chem. Soc.* **1992**, *114*, 5832−5842.
(58) Longo, P.; Grassi, A.; Pellecchia, C.; Zambelli, A. *Macromolecules* **1987**, *20*, 1015−1018.
(59) Dahlmann, M.; Erker, G.; Nissinen, M.; Fröhlich, R. *J. Am. Chem. Soc.* **1999**, *121*, 2820−2828.
(60) Resconi, L.; Fait, A.; Piemontesi, F.; Colonnesi, M.; Rychlicki, H.; Zeigler, R. *Macromolecules* **1995**, *28*, 6667−6676.
(61) Busico, V.; Cipullo, R. *J. Am. Chem. Soc.* **1994**, *116*, 9329−9330.
(62) Leclerc, M. K.; Brintzinger, H. H. *J. Am. Chem. Soc.* **1995**, *117*, 1651−1652.
(63) Leclerc, M. K.; Brintzinger, H. H. *J. Am. Chem. Soc.* **1996**, *118*, 9024−9032.
(64) Busico, V.; Caporaso, L.; Cipullo, R.; Landriani, L.; Angelini, G.; Margonelli, A.; Segre, A. L. *J. Am. Chem. Soc.* **1996**, *118*, 2105−2106.
(65) Busico, V.; Cipullo, R.; Caporaso, L.; Angelini, G.; Segre, A. L. *J. Mol. Catal. A: Chem.* **1998**, *128*, 53−64.
(66) Busico, V.; Cipullo, R. *Prog. Polym. Sci.* **2001**, *26*, 443−533.
(67) Chien, J. C. W.; Tsai, W. M.; Rausch, M. D. *J. Am. Chem. Soc.* **1991**, *113*, 8570−8571.
(68) Schmid, M.; Eberhardt, R.; Klinga, M.; Leskelä, M.; Rieger, B. *Organometallics* **2001**, *20*, 2321−2330.

DOI: 10.1021/acs.organomet.6b00814
Organometallics XXXX, XXX, XXX−XXX